26 December 1997

ELSEVIER

Chemical Physics Letters 281 (1997) 343–351

CHEMICAL PHYSICS LETTERS

Multi-dimensional entropy sampling Monte Carlo method and free energy landscape of Ar_{13}

GuanHua Chen, Guang-Wen Wu

Department of Chemistry, The University of Hong Kong, Pokfulam Road, Hong Kong, Hong Kong

Received 12 August 1997; in final form 17 October 1997

Abstract

A multi-dimensional entropy sampling Monte Carlo method is proposed and implemented to evaluate directly the entropy of a 13-atom argon cluster (Ar_{13}). The Helmholtz free energy of the cluster is obtained and expressed as a function of the cluster's energy E and radius of gyration R_{gy} at several temperatures. A transition zone where the accessible range of R_{gy} varies rapidly is found to be the coexistence region of the solid-like and liquid-like structures. © 1997 Elsevier Science B.V.

1. Introduction

Helmholtz Free energy is an important thermodynamic quantity. It determines the equilibrium properties of a system, and dictates the relations among its structure, dynamics and energy. Molecular dynamics and Monte Carlo methods have been utilized to calculate Helmholtz free energies of various systems [1–5]. The resulting free energies were generally expressed as functions of a parameter of the systems, e.g. energy or some conformational parameter. These one-dimensional functions provide useful but sometime limited information on structures and dynamics. Recently an entropy sampling Monte Carlo (ESMC) method was developed to determine Helmholtz free energy as a function of the energy [6]. It has been applied to spin glasses and proteins [6–10]. Two- or multi-dimensional free energy functions contain obviously much more information. It would be highly desirable to have an efficient algorithm to calculate a multi-dimensional free energy function of a system.

The Metropolis Monte Carlo method [19] simulates canonical ensembles in which the probability of occurrence of a conformation x obeys the Boltzmann distribution:

$$p(x) \propto e^{-\beta E}, \tag{1}$$

where $E(x)$ is the energy of the conformation x, and $\beta = 1/k_B T$ with T being the temperature and k_B being the Boltzmann constant. The ESMC method [6], however, is based on an artificial distribution which is determined by the entropy S. Specifically, denote $S(E)$ as the entropy function of the energy E, the probability of occurrence of a conformation x is as follows [6,8],

$$p(x) \propto e^{-S[E(x)]/k_B}. \tag{2}$$

This leads to a one-dimensional random walk for energy E, i.e. the probability distribution with respect to the energy E is

$$P(E) \propto N(E) e^{-S[E]/k_B} = e^{S(E)/k_B} e^{-S(E)/k_B} = 1. \tag{3}$$

where $N(E)$ is the spectral density of states, and $N(E) = e^{S(E)/k_B}$. The probabilities of occurrence for all values of E are the same. The ESMC method

PII S0009-2614(97)01222-0

ensures that the system can overcome any energy barrier and may help solve the quasi-ergodicity problem. $S(E)$ is unknown before the simulation, and is determined through iterations. Helmholtz free energy F at a temperature T may be readily obtained using the thermodynamic relation $F(E) = E - TS(E)$. Since the resulting entropy and free energy are one-dimensional functions of the energy, we refer this method as the one-dimensional entropy sampling Monte Carlo (1D-ESMC) method. The 1D-ESMC method may be generalized to calculate multi-dimensional entropy and free energy [6].

Argon clusters have attracted a considerable amount of research effort [11–17]. Melting transition, Rydberg states of an argon atom, separation of bulk and surface features, and microscopic origins of macroscopic properties have been investigated extensively [13–16]. To understand growth and nucleation, free energies of clusters with different number of atoms have been calculated [12,17]. A 13-atom argon cluster Ar_{13} is a very stable cluster. The structure of its ground state is an icosahedron [18] and thus, naturally, of rigid, solid-like form. It was found that at a temperature $T = 34$ K the solid-like structure melts to a non-rigid, liquid-like form [14].

In this manuscript we present a multi-dimensional entropy sampling Monte Carlo (mD-ESMC) method to evaluate multi-dimensional entropy and free energy functions, and apply this method to an Ar_{13}. The resulting entropy and free energy are expressed as two-dimensional functions of the cluster's energy E and radius of gyration R_{gy}. The implications of the entropy and free energy functions on the equilibrium structure and dynamics are discussed.

Let us imagine a system which can be characterized by its energy E and order parameters A, Q, D and others. The order parameters may be, for instance, the size of a system, the number of hydrogen bonds, and the portions of α-helices and β sheets. Its free energy at a temperature T can be expressed as

$$F(E,A,Q,D,\cdots) = E - TS(E,A,Q,D,\cdots), \tag{4}$$

where $\cdots$ denotes any other relevant order parameters, and $F(E,A,Q,D,\cdots)$ and $S(E,A,Q,D,\cdots)$ are the free energy and entropy as functions of E, A, Q, D and $\cdots$, respectively. If the probability of occurrence of a conformation x is defined as,

$$p(x) \propto e^{-S[E(x),A(x),Q(x),D(x),\cdots]/k_B}, \tag{5}$$

the distribution function with respect to E, A, Q, D and the other order parameters is then

$$P(E,A,Q,D,\cdots) \propto N(E,A,Q,D,\cdots)\, e^{-S(E,A,Q,D,\cdots)/k_B} = 1, \tag{6}$$

where $N(E,A,Q,D,\cdots)$ is the density of conformation at E, A, Q, D and $\cdots$, and $N(E,A,Q,D,\cdots) = e^{S(E,A,Q,D,\cdots)/k_B}$. In another word, the probabilities of occurrence for all values of E, A, Q, D and the other order parameters are equal. Eq. (6) may be employed as a criteria to decide the convergence of $S(E,A,Q,D,\cdots)$. A Markovian chain with transition probabilities

$$\frac{\pi(x \to x')}{\pi(x' \to x)} = \frac{\exp\{-S[E(x'),A(x'),Q(x'),D(x'),\cdots]/k_B\}}{\exp\{-S[E(x),A(x),Q(x),D(x),\cdots]/k_B\}} \tag{7}$$

leads to the distribution described by Eq. (6). Here x and x' are a pair of conformations in the Markovian chain, and $\pi(x \to x')$ and $\pi(x' \to x)$ are the transition probabilities for x to x' and x' to x, respectively.

Since $S(E,A,Q,D,\cdots)$ is unknown before the simulation, a function $J(E,A,Q,D,\cdots)$ is introduced as an approximation to the entropy function $S(E,A,Q,D,\cdots)$, and the probability of occurrence of a conformation x is then taken as

$$p(x) \propto e^{-J(E,A,Q,D,\cdots)/k_B}. \tag{8}$$

An mD-ESMC simulation consists many iterations, and each iteration has many steps. During each step, a trial conformation is generated, and chosen or discarded according to the probability of occurrence, Eq. (8). In the beginning of a simulation, $J(E,A,Q,D,\cdots)$ is set to zero. During an iteration, the ranges of E, A, Q, D and $\cdots$ are divided into discrete increments ΔE, ΔA, ΔQ, ΔD and $\cdots$, respectively. A multi-dimensional histogram $H(E,A,Q,D,\cdots)$ is recorded for the number of visits to conformations within $(E, E+\Delta E)$, $(A, A+\Delta A)$, $(D, D+\Delta D)$ and $\cdots$. $J(E,A,Q,D,\cdots)$ is updated at the end of the iteration according to the

following formula:

$$J_{\text{new}}(E,A,Q,D,\cdots) = J_{\text{old}}(E,A,Q,D,\cdots) + \log\{H(E,A,Q,D,\cdots)\}, \quad (9)$$

where $J_{\text{old}}(E,A,Q,D,\cdots)$ and $J_{\text{new}}(E,A,Q,D,\cdots)$ are the values of the function $J(E,A,Q,D,\cdots)$ at E, A, Q, D and the other order parameters for current and next iterations, respectively. In case that $H(E,A,Q,D,\cdots)$ is zero, $H(E,A,Q,D,\cdots)$ is taken to be one. When the histogram $H(E,A,Q,D,\cdots)$ at the end of a particular iteration is flat with respect to E, A, Q, D and $\cdots$, $J(E,A,Q,D,\cdots)$ is then converged, and the relative entropy function $S(E,A,Q,D,\cdots) = J(E,A,Q,D,\cdots)$.

The average values of E, A, Q, and D can be evaluated directly from the free energy function $F(E,A,Q,D,\cdots)$. For instance, the average value of A can be calculated using

$$\langle A\rangle = \frac{\sum A e^{-\beta F(E,A,Q,D,\cdots)}}{\sum e^{-\beta F(E,A,Q,D,\cdots)}}, \quad (10)$$

where $\sum$ is a summation over all the values of E, A, Q, D and $\cdots$.

We apply the mD-ESMC method to an Ar_{13}. The interaction between two argon atoms are described by a Lennard-Jones potential,

$$V(r) = 4\epsilon\left[(\sigma/r)^{12} - (\sigma/r)^{6}\right], \quad (11)$$

where $\epsilon = 1.67\times10^{-21}$ J, $\sigma = 3.4\times10^{-10}$ m [14], and r is the distance between the two atoms. The 13 atoms are confined in a cube with its edge $a = 6.38\sigma$. The initial positions of 13 atoms are selected randomly.

The radius of gyration R_{gy} measures the size of the cluster, and reflects its structure. It is defined as follows.

$$R_{\text{gy}} = \sqrt{\frac{1}{N}\sum_{i=1}^{N}(\boldsymbol{R}_i - \boldsymbol{R}_{\text{cm}})^2}, \quad (12)$$

where $N = 13$ is the number of atoms, $\boldsymbol{R}_i$ is the displacement of vector of the i-th atom, and $\boldsymbol{R}_{\text{cm}}$ is the displacement of vector of the center of the masses. A two-dimensional ESMC (2D-ESMC) method is employed to evaluate its entropy and free energy as functions of its energy E and R_{gy} at different temperatures. We refer the space spanned by the values of E and R_{gy} as the phase space. The free energy function at T can be expressed as

$$F(E,R_{\text{gy}}) = E - TS(E,R_{\text{gy}}). \quad (13)$$

A new conformation is generated by moving each of the 13 argon atoms during a step, and each move is decided by three random numbers. It is observed that with such a strategy the system rarely visits its low energy conformations. A conformation-biased strategy is used instead. A temperature T_{g} is introduced, and the conformation x'' after an new move is chosen according to a Boltzmann distribution,

$$w(x'') \propto e^{-E(x'')/k_{\text{B}}T_{\text{g}}}. \quad (14)$$

The bias is applied so that the low energy conformations are selected more favorably as trial conformations. T_{g} is set to 1.0ϵ in our simulation. Consequently, the transition probability between a pair of conformation x and x' in the Markovian chain must be corrected. The corrected transition probabilities satisfy

$$\frac{\pi(x\to x')}{\pi(x'\to x)} = \frac{\exp\{-J[E(x'),R_{\text{gy}}(x')]/k_{\text{B}}\}\exp[E(x')/k_{\text{B}}T_{\text{g}}]}{\exp\{-J[E(x),R_{\text{gy}}(x)]/k_{\text{B}}\}\exp[E(x)/k_{\text{B}}T_{\text{g}}]}. \quad (15)$$

During the simulation, a two-dimensional histogram $H(E,R_{\text{gy}})$ is recorded for each iteration. The ranges of E and R_{gy} are taken as $(-50\epsilon,0)$ and $(0,6.38\sigma)$, respectively. Both ranges are evenly divided into 50 segments, and thus, the phase space is partitioned into 2500 small squares. The increments for E and R_{gy} are $\Delta E = 1.0\epsilon$ and $\Delta R_{\text{gy}} = 0.128\sigma$, respectively. Thus, the histogram $H(E,R_{\text{gy}})$ becomes a 50×50 matrix. When the distribution of this two-dimensional histogram becomes flat, a convergence is achieved, and the simulation ends. After the simulation, the final $J(E,R_{\text{gy}})$ is taken to be the relative entropy $S(E,R_{\text{gy}})$, i.e. $S(E,R_{\text{gy}}) \equiv J(E,R_{\text{gy}})$. There are 10^7 steps per iteration, and 50 iterations per simulation. The relative free energies from $T = 0.2\epsilon$ to 0.38ϵ are evaluated according to Eq. (13). Finally, the average energy $\langle E\rangle$ and radius of gyration $\langle R_{\text{gy}}\rangle$ are calculated for the above temperature

range. To examine the reliability of our simulation, we carry out the conventional Metropolis Monte Carlo simulation [19] at $T/\epsilon = 0.2$, 0.3 and 0.35 with 5×10^5 steps per simulation. The resulting average energy and radius of gyration are compared with those of the 2D-ESMC simulation.

In Fig. 1, we plot the relative entropy S versus the energy E and the radius of gyration R_{gy}. There is a flat sheet at the plane $S = 0$. Any point on the sheet is out of the phase space. Thus, the sheet does not have any physical meanings and is for guidance to one's eyes only. Generally, as E decreases, the entropy decreases as well. This is consistent with the physical intuition: as E lowers its value, the cluster becomes smaller and the accessible physical space decreases, i.e. the entropy decreases. It is noted that the maximum value of the entropy is at $(E = -1.5\epsilon, R_{gy} = 3.13\sigma)$, which is not at the highest energy line. It is because that the cube in the simulation has its finite size. As the cluster grows bigger, some atoms eventually hit the walls of the cube and can not access some conformations which have the same energy as that of the smaller conformations. The entropy assumes its maximum values near the lowest R_{gy} values when $-44 < E/\epsilon < -30$; and when $E/\epsilon > -30$, the entropy increases first and then decreases as R_{gy} increases. The entire landscape resembles a high plateau descending towards the region of low E value. A ridge exists close to the edge of the landscape when $E/\epsilon < -30$ and then bends slowly but steadily towards larger R_{gy} as E increases. The contour illustrates clearly this phenomena. The accessible range of R_{gy} increases first as E is lowered from zero, and is virtually unchanged for $-30\epsilon < E < -8\epsilon$. Then the accessible range shrinks rapidly when E varies from -33ϵ to -39ϵ. We call the region i.e. -33ϵ to -39ϵ the transition zone. The rapid change corresponds a zigzag edge along the up-right edge of the transition zone. The rough feature of the edge indicates sudden changes of the cluster's structure and implies the appearance of different solid-like structures in the transition zone. Note that there are some sharp inverted peaks along the edges. For small squares along the edges, some of their areas are beyond the boundaries of the phase space. This leads smaller values of entropy at the edges. Sometimes only tiny portion of a square is accessible, and this leads to a very small value of S for the square.

To estimate the statistical errors in the simulated

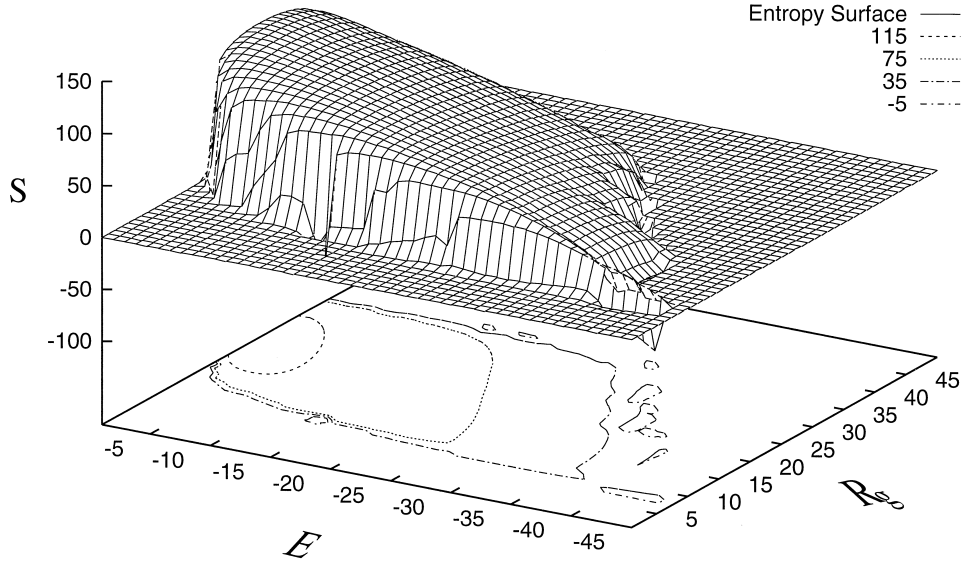

Fig. 1. Two-dimensional entropy surface: S versus E and R_{gy}. The units of S, E and R_{gy} are k_B, ϵ and 0.128σ, respectively. The flat sheet at $S = 0$ does not have any physical meanings.

entropy, we follow Hao and Scheraga by measuring the variances of the entropy in the last eight iterations. The standard deviation, $\mathrm{SD}(E,R_{\mathrm{gy}})$, of the entropy $S(E,R_{\mathrm{gy}})$ is estimated as follows:

$$\mathrm{SD}(E,R_{\mathrm{gy}}) = \sqrt{\langle \Delta S(E,R_{\mathrm{gy}})^2 \rangle - \langle \Delta S(E,R_{\mathrm{gy}}) \rangle^2} \tag{16}$$

where $\Delta S(E,R_{\mathrm{gy}})$ is the increment of the entropy $S(E,R_{\mathrm{gy}})$ of one iteration with respect to that of previous one, and $\langle \cdots \rangle$ represents the average over all the eight iterations. Fig. 2 shows $\mathrm{SD}(E,R_{\mathrm{gy}})$ as a function of E and R_{gy}. Obviously the deviations along the edges are quite large, which is about 3.0 to 6.0; while the deviations in the rest of the phase space are between 0.1 and 0.3.

In Fig. 3, we plot the relative free energy F versus the energy E and the radius of gyration R_{gy} for the temperatures $T/\epsilon = 0.2$, 0.3 and 0.4. The large variation of $S(E,R_{\mathrm{gy}})$ along the edges leads to substantial fluctuations of $F(E,R_{\mathrm{gy}})$ in the area. Compared to that of the edges, the free energy landscape is rather flat in the rest of the phase space. The free energy in some areas along the edges is very large and contributes little to the thermodynamic properties of the cluster. The free energy surface in these areas is, therefore, not included in the figure, and is replaced by smooth sheets on the boundary, see Fig. 3. These sheets also cover the same unphysical space as those in Fig. 1. The corresponding contour is plotted as well. The three free energy surfaces resemble three basins. At $E = 0$, the widths of the basins along the R_{gy} axis are quite large, and the accessible values of R_{gy} are between 2.30σ and 4.72σ. The widths decrease dramatically in the transition zone. At $E = -43.5\epsilon$, the accessible values of R_{gy} are only between 1.02σ and 1.15σ. Generally, the free energy surfaces are higher at large R_{gy}, particularly when E is not very large. This is because that large R_{gy} corresponds to elongated conformations which has less flexibility. A valley exists at the lower-right corner of each of the basins. As E increases, the valleys merge into the bottoms of the basins and disappear. The valleys correspond to the conformations of a tightly packed cluster. At $T = 0$, $F(E,R_{\mathrm{gy}}) = E$, i.e. the free energy surface is a plane. Among the three surfaces, the free energy landscape at $T = 0.2\epsilon$ is quite flat and its basin is shallow. This is because that T is small, the energy dominates the characteristics of the surface. As T increases, the effect of the entropy becomes important, the basin appears deeper, and its curvature increases. At $T = 0$, the minimum point of the free energy function ($E = -43.5\epsilon$, and $R_{\mathrm{gy}} = 1.08\sigma$) corresponds to the minimum energy icosahedral structure. At $T/\epsilon = 0.2$, 0.3 and 0.4, the minimum point is at ($E = -40.5\epsilon$, $R_{\mathrm{gy}} = 1.08\sigma$), ($E =$

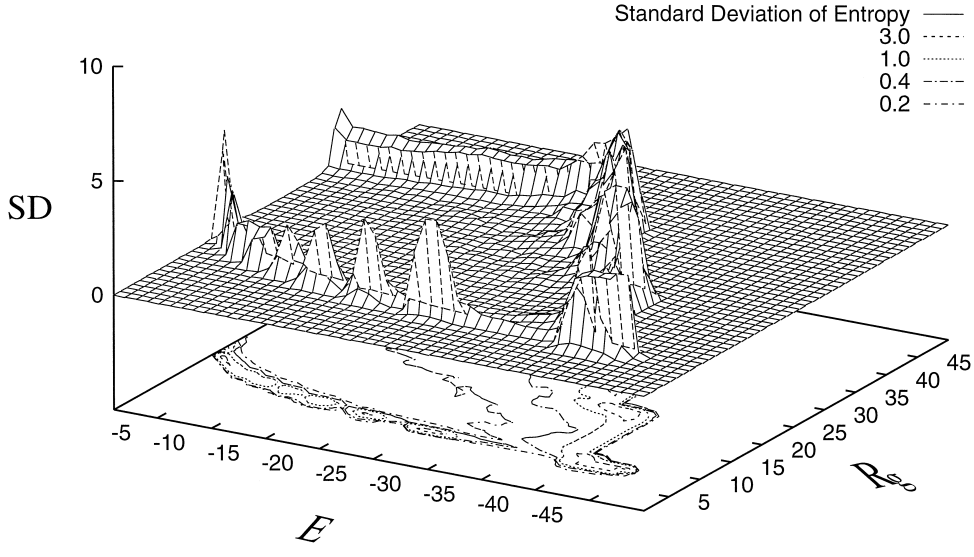

Fig. 2. Estimated standard deviations of relative entropy. SD, E and R_{gy} are in units of k_{B}, ϵ and 0.128σ, respectively.

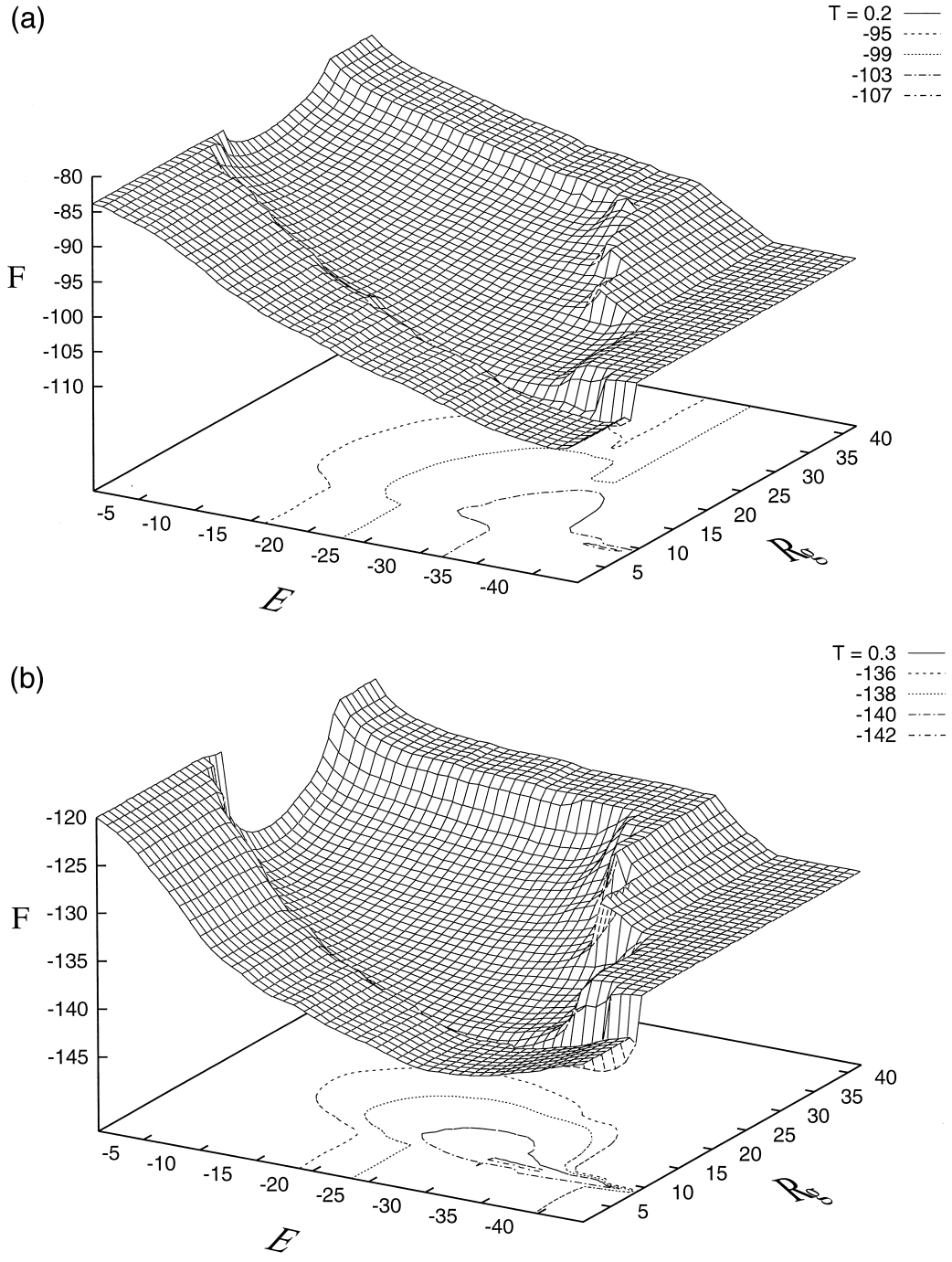

Fig. 3. Free energy landscape: F versus E and R_{gy}. The units of F, E and R_{gy} are ϵ, ϵ and 0.128σ, respectively. Smooth sheets on the boundary do not have any physical meanings.

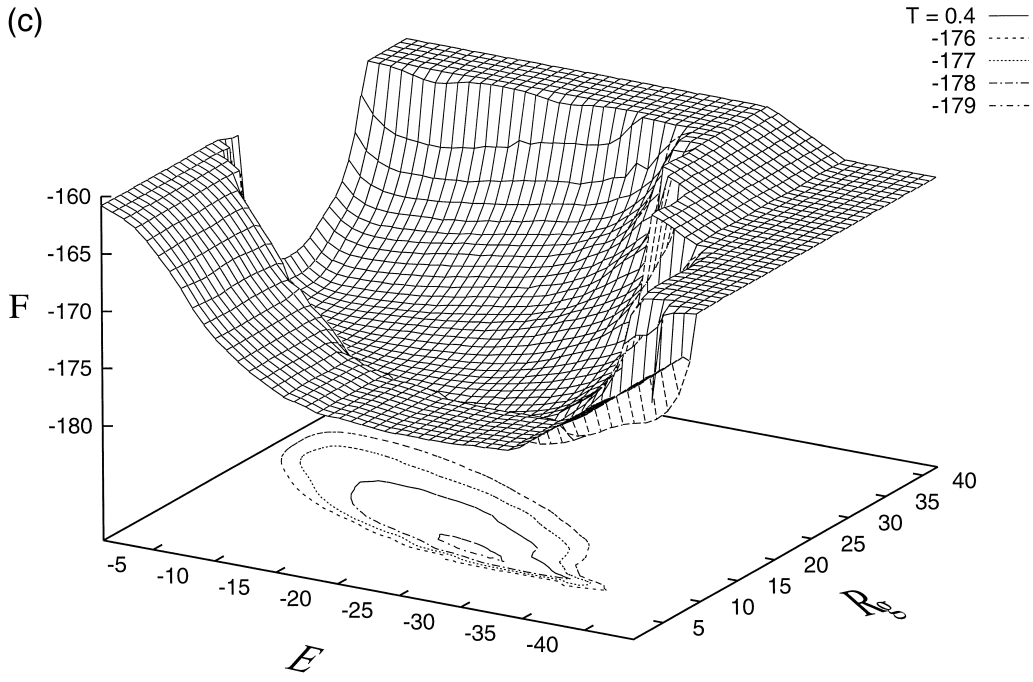

Fig. 3 (continued).

-32.5ϵ, $R_{gy} = 1.21\sigma$) and ($E = -26.5\epsilon$, $R_{gy} = 1.34\sigma$), respectively. As $T \to \infty$, the entropy dominates, and the minimum is at ($E = -1.5\epsilon$, $R_{gy} = 3.13\sigma$). The location of the free energy minimum moves to the regions of higher E and larger R_{gy} as the temperature rises, and the trajectory is along the ridge of the entropy plateau, see Fig. 1. The movement of the free energy minimum reflects the fact that as the temperature increases the system acquires more energy and its size becomes larger. The movement along the R_{gy} axis is rather slow when $E < -30\epsilon$. Overall the free energy surfaces are smooth, which implies that there is no barrier for the cluster to find its thermodynamic equilibrium conformations.

The average energy $\langle E \rangle$ and radius of gyration $\langle R_{gy} \rangle$ versus temperature T are plotted in Fig. 4. $\langle E \rangle$ and $\langle R_{gy} \rangle$ are obtained according to Eq. (10) by substituting the relative free energy functions at the corresponding temperatures. In Fig. 4a, there is a change of the slope at $T/\epsilon \approx 0.28$. Since the specific heat C_v is simply the derivative of $\langle E \rangle$ with respect to temperature T, i.e. $C_v = \mathrm{d}\langle E \rangle / \mathrm{d}T$, there should be a peak for C_v at $T \approx 0.28\epsilon = 34$ K. This specific heat peak corresponds to a transition between a rigid, solid-like structure and a non-rigid, liquid-like structure [14,20]. To check the validity of our results, we compare $\langle E \rangle$ and $\langle R_{gy} \rangle$ with the results of a Metropolis Monte Carlo simulation, see Fig. 4. The Metropolis Monte Carlo simulation is carried at $T/\epsilon = 0.2$, 0.3 and 0.35. The comparison is satisfactory.

Berry and coworkers [14] found that the magnitude of the root-mean-square bond length fluctuation changes four times at the melting temperature 34 K. During the melting, solid-like and liquid-like forms coexist, which leads to so-called coexistence region. The total energy of coexistence region varies from -4.4×10^{-14} to -3.7×10^{-14} erg/atom. The lower and upper energy boundaries of the transition zone is -39ϵ and -33ϵ, respectively. These two energy boundaries correspond to the total energies of -4.41×10^{-14} and 3.65×10^{-14} erg/atom, respectively. Therefore, we conclude that the solid-like and liquid-like structures coexist in the transition zone. Below the transition zone ($E < -39\epsilon$), the cluster is solid-like. And above the transition zone ($E > -33\epsilon$), the system is liquid-like. At the melting temperature, the free energy minimum is at ($E =$

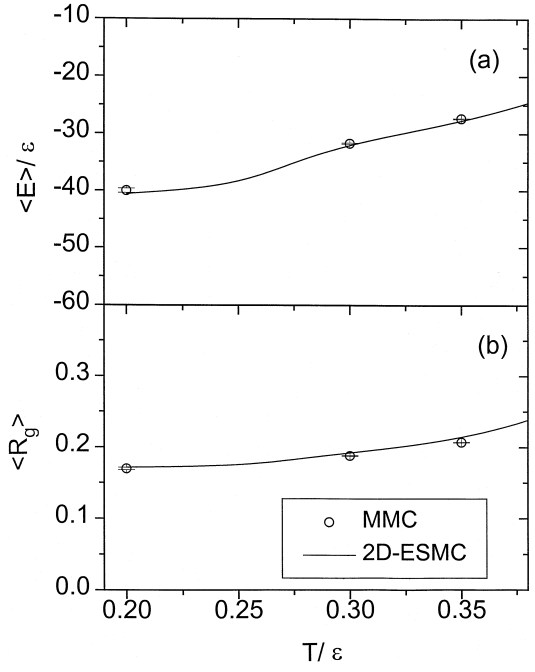

Fig. 4. (a) Average energy $\langle E \rangle$ versus temperature T. (b) Average radius of gyration $\langle R_{gy} \rangle$ versus temperature T. The solid lines are the results of the 2D-ESMC simulations, and the open circles are the results of the Metropolis Monte Carlo (MMC) simulations. The units of $\langle E \rangle$, $\langle R_{gy} \rangle$ and T are ϵ, 0.128σ and ϵ, respectively. MMC stands for Metropolis Monte Carlo.

$-33\epsilon, R_{gy} = 1.2\sigma$), and locates at the upper boundary of the transition zone.

In the space spanned by the order parameters, there are some regions where S is large and other regions where S is small. In the regions where the entropy is large, the values of S can be determined with a reasonable amount of computer resource, and while much more resource is required to evaluate the entropy for the same amount of area in the regions where the entropy is very small. If the entropies of the two kinds of regions are to be calculated simultaneously, much computer time will be wasted in the regions of large S. The efficiency can be improved by dividing the space into two or more different regions where simulations are carried out separately. Adjacent regions should overlap with each other so that the relative entropy among them may be determined. The regions should be divided such that the overall computational time is minimum. In our simulation we found that large amount of computer time is required to determine the relative entropy per square in the region where $E < -39\epsilon$. We thus carried a separate simulation by restricting the energy of Ar_{13} below -38ϵ. The simulation consists of 50 iterations and each iteration has 5×10^6 steps. In Hao and Scheraga's work T_g was chosen by the formula $\beta_g = dS(E)/dE$ where $\beta_g = 1/k_B T_g$. We find that $T_g = 1.0\epsilon$ leads to a good result and an adequate amount of computation time. The compution time of an mD-ESMC simulation is proportional to the volume of its parameters' space. If the same number N of increments is employed for all parameters, the computation time scales as N^d, where d is the number of parameters. Compared with other Monte Carlo methods [12,21–23], the mD-ESMC method is convenient in implementation and capable to yield the multi-dimensional entropy and free energy surfaces during one simulation. Two- or multi-dimensional free energy landscape provides much richer information than that of one-dimensional free energy curve. Ar_{13} is relatively small. The mD-ESMC method may be applied to much more complex systems, for instance, protein. The free energy landscapes of proteins are expected to possess many special features [24]. These features may help reveal the secrets of protein folding: how do proteins manage to find their native conformations in such a short time? Energy, helicity, radius of gyration and number of native contacts may be proper variables to characterize protein free energy landscape.

In summary, a mD-ESMC method is proposed and implemented to calculate multi-dimensional entropy and free energy. A two-dimensional entropy $S(E, R_{gy})$ and free energy $F(E, R_{gy})$ of an argon cluster Ar_{13} is obtained. The resulting free energy landscapes provide important information about the structure and dynamics of the cluster. This method is of wide applicability, and may be applied to a variety of complex and interesting systems.

Acknowledgements

The authors wish to thank Dr. YiJing Yan for proof-reading. The support of the committee on re-

search and conference grants of the University of Hong Kong is gratefully acknowledged.

References

[1] J.P. Valleau, G.M. Torrie, in: B.J. Berne (Ed.), Statistical Mechanics, Part A, Plenum Press, New York, 1977.
[2] D.L. Beveridge, F.M. DiCapua, Annu. Rev. Biophys. Biophys. Chem. 18 (1989) 431.
[3] E.M. Boczko, C.L. Brooks III, Science 269 (1995) 393.
[4] W.L. Jorgensen, J. Phys. Chem. 87 (1983) 5304.
[5] K. Binder, in: K. Binder (Ed.), Monte Carlo Methods in Statistical Physics, Springer, Berlin, 1986.
[6] J. Lee, Phys. Rev. Lett. 71 (1993) 211.
[7] U.H.E. Hansmann, Y. Okamoto, J. Comp. Chem. 14 (1993) 1333.
[8] M.-H. Hao, H.A. Scheraga, J. Phys. Chem. 98 (1994) 4940.
[9] A. Kidera, Proc. Natl. Acad. Sci., USA 92 (1995) 9886.
[10] A. Kolinski, W. Galazka, J. Skolnick, Proteins 26 (1996) 271.
[11] H. Haberland, Clusters of Atoms and Molecules: Theory, Experiment, and Clusters of Atoms, Springer Series in Chemical Physics, Vol. 52, Springer, Berlin, 1994, and references therein.
[12] J.K. Lee, J.A. Barker, F.F. Abraham, J. Chem. Phys. 58 (1973) 3166.
[13] J. Farges, M.F. de Faraudy, B. Raoult, G. Torchet, J. Chem. Phys. 78 (1983) 5067.
[14] T.L. Beck, J. Hellinek, R.S. Berry, J. Chem. Phys. 84 (1986) 2783.
[15] R. Chitra, S. Yashonath, J. Phys. Chem. B 101 (1997) 389.
[16] L.L. Boyer, J.Q. Broughton, Phys. Rev. B 42 (1990) 11461.
[17] C.L. Weakliem, H. Reiss, J. Chem. Phys. 99 (1993) 5374.
[18] M.R. Hoare, P. Pal, Adv. Phys. 20 (1971) 161.
[19] N. Metropolis, A.W. Rosebluth, M.N. Rosenbluth, A.H. Teller, E. Teller, J. Chem. Phys. 21 (1953) 1087.
[20] G.H. Chen, N. Karasawa, W.A. Goddard III, unpublished.
[21] B.A. Berg, T. Neuhaus, Phys. Rev. Lett. 68 (1992) 9.
[22] A.M. Ferrenberg, R.H. Swendsen, Phys. Rev. Lett. 63 (1989) 1195.
[23] K.-C. Lee, J. Phys. A 23 (1990) 2087.
[24] H. Frauenfelder, S.G. Sligar, P.G. Wolynes, Science 254 (1991) 1598.